Original Investigation

Value of Dual-Energy CT-Derived Metrics for the Prediction of Bone Non-union in Distal Radius Fractures

Philipp Reschke, MD, Jennifer Gotta, MD, Adrian Stahl, Vitali Koch, MD, Christoph Mader, MD, Simon S. Martin, MD, Jan-Erik Scholtz, MD, Christian Booz, MD, Ibrahim Yel, MD, Daniel A. Hescheler, MD, Tatjana Gruber-Rouh, MD, Katrin Eichler, MD, Thomas J. Vogl, MD, Leon D. Gruenewald, MD

Rationale and Objectives: Bone non-union is a serious complication of distal radius fractures (DRF) that can result in functional limitations and persistent pain. However, no accepted method has been established to identify patients at risk of developing bone non-union yet. This study aimed to compare various CT-derived metrics for bone mineral density (BMD) assessment to identify predictive values for the development of bone non-union.

Materials and Methods: CT images of 192 patients with DRFs who underwent unenhanced dual-energy CT (DECT) of the distal radius between 03/2016 and 12/2020 were retrospectively identified. Available follow-up imaging and medical health records were evaluated to determine the occurrence of bone non-union. DECT-based BMD, trabecular Hounsfield unit (HU), cortical HU and cortical thickness ratio were measured in normalized non-fractured segments of the distal radius.

Results: Patients who developed bone non-union were significantly older (median age 72 years vs. 54 years) and had a significantly lower DECT-based BMD (median 68.1 mg/cm^3 vs. 94.6 mg/cm^3, $p < 0.001$). Other metrics (cortical thickness ratio, cortical HU, trabecular HU) showed no significant differences. ROC and PR curve analyses confirmed the highest diagnostic accuracy for DECT-based BMD with an area under the curve (AUC) of 0.83 for the ROC curve and an AUC of 0.46 for the PR curve. In logistic regression models, DECT-based BMD was the sole metric significantly associated with bone non-union.

Conclusion: DECT-derived metrics can accurately predict bone non-union in patients who sustained DRF. The diagnostic performance of DECT-based BMD is superior to that of HU-based metrics and cortical thickness ratio.

Key Words: Bone density; Pseudarthrosis; Osteoporosis; Bone diseases; Computed tomography.

INTRODUCTION

Distal radius fractures (DRF) are amongst the most commonly observed fractures, accounting for up to 18% in elderly patients (1). In ageing western populations, the rate of DRFs is expected to continue to rise. DRFs cause substantial healthcare costs. A major risk factor for complicated DRFs is osteoporosis (2,3). Bone non-union is a rare but serious complication of DRF that can lead to pain and limitations in range of motion, grip strength, and dexterity. Thus, this medical condition often results in a considerable personal burden for the patient (4).

Multiplanar CT is the gold standard for preoperative planning as it adds valuable information about the degree of displacement, fragmentation and associated intra-articular involvement. By visualizing the displaced fracture in three dimensions, surgeons tend to have a better understanding of the fracture geometry and therefore might optimize the surgical approach (5).

Quantitative CT (QCT) is a precise method for evaluating the volumetric bone mineral density (BMD) of trabecular bone. However, it is typically not feasible to apply QCT

Acad Radiol xxxx; xx:xxx–xxx

From the Department of Diagnostic and Interventional Radiology, Hospital of the Goethe University Frankfurt, Frankfurt am Main, Germany (P.R., J.G., A.S., V.K., C.M., S.S.M., J.-E.S., C.B., I.Y., T.G.-R., K.E., T.J.V., L.D.G.); Department of Radiology and Nuclear Medicine, University Hospital Magdeburg, Magdeburg, Germany (D.A.H.). Received December 13, 2023; revised January 14, 2024; accepted January 30, 2024. **Address correspondence to**: P.R. e-mail: P.Reschke@med.uni-frankfurt.de

https://doi.org/10.1016/j.acra.2024.01.041

retrospectively because it necessitates an accurately placed in-scan calibration phantom below the patient. A calibration phantom is a standardized object mimicking bone composition which enables to convert HU measurements into accurate BMD measurements (6). To address this constraint, alternative opportunistic BMD assessment methods, such as trabecular HU, cortical HU and cortical thickness ratio have been proposed (7–9). These methods provide only indirect indications of bone quality without assessing the physical bone density. As a consequence, HU-based assessments suffer from several limitations such as overlying tissue distortion, changes in body composition, scan setting variability and CT model differences (10,11). Inadequate scan resolution, for example, can cause a partial volume effect, resulting in underestimation of bone density (12). Variations in the cortical thickness ratio may complicate the interpretation of the results. The cortical thickness ratio can be affected by factors like gender, and exercise (13,14).

The dual-energy CT (DECT) uses a range of X-ray spectra allowing material differentiation retrospectively. A DECT-based postprocessing algorithm assesses volumetric BMD BMD via material decompensation. In comparison to QCT, the utilization of a phantom during the examination is no longer needed. The algorithm's feasibility was demonstrated when applied to routine examinations (15–18). Recent studies have shown that it provides superior diagnostic accuracy for identifying osteoporosis compared to HU-based assessment methods (19). In spite of that, DECT scanners are not widely available due to high acquisition costs (20). Our goal was to evaluate if opportunistic BMD assessments are reliable alternatives to predict bone non-union.

We hypothesized that the diagnostic accuracy of DECT-based BMD assessment in predicting bone non-union in DRF patients is higher than than that of opportunistic BMD assessments.

MATERIALS AND METHODS

The institutional review board approved this retrospective study and waived the requirement to obtain written informed consent.

Patient Selection

DECT examinations of radius fractures were retrospectively acquired between 03/2016 and 12/2020 through the internal picture archiving and communication system (PACS) at the XXX. The inclusion criteria consisted of DRF patients aged 18 years or older who had undergone a non-contrast DECT of the radius. The exclusion criteria were severe destruction of the distal radius, suspected or known malignancy, metallic implants, osteomalacia, and the unavailability of patient health records. The final study population consisted of 192 patients in total **(**Fig 1**).**

Image Protocol

To conduct CT examinations of the radius, a third-generation dual-source CT device (SOMATOM Force; Siemens Healthineers) was employed in dual-energy mode. The X-ray tubes were operated at different kilovolt (kV) settings (tube 1: 90 kVp, 180 mAs, tube 2: Sn150 kVp 8 [0.64 mm tin filter], 180 mAs). Image series were acquired in a craniocaudal direction. Patients were lying face down with their arm extended over the head. The forearm and wrist were kept in a natural position. No contrast agent was administered during the examinations. The system utilized automatic tube current modulation (CARE dose 4D; Siemens Healthineers).

Image Reconstruction

During each CT examination, three sets of images were acquired: one at 90 kVp, another at Sn150 kVp, and a weighted average set with a ratio of 0.5:0.5. Axial, coronal, and sagittal image series were reconstructed with a specialized dual-energy bone kernel (Br69f), following institutional guidelines. The thickness of the image slices was 1 mm with an increment of 0.75 mm. Subsequently, all image series were transferred to the PACS (General Electric Company).

Image Interpretation

Two radiologists with 14 and six years of experience in musculoskeletal imaging independently carried out HU-based bone density assessments and cortical thickness ratio using preoperative CT images of the DRF. Furthermore, they independently assessed all obtained CT images using the AO Foundation's and Orthopaedic Trauma Association's (AO/OTA) classification system for radius fractures (21). Both radiologists were blinded to clinical symptoms and injury mechanisms. In cases where there were divergent assessments, a third radiologist with 10 years of experience in musculoskeletal imaging was consulted. The majority decision was reported. Surgical reports, electronic patient files and patient radiographs were evaluated for the occurrence of bone non-union. Bone non-union was defined as the presence of a fracture persisting for at least nine months without signs of healing for three months, as observed in CT scans.

Phantomless BMD Assessment

Volumetric BMD assessment was carried out manually by a single board-certified radiologist with seven years of experience in musculoskeletal imaging. The delineation of the three-dimensional region of interest (ROI) of the non-fractured segments of the DRF was performed as previously reported (22). Both DECT image series were used as input for phantomless volumetric BMD evaluation with dedicated software (BMD Analysis, Fraunhofer IGD, Germany). This software uses a material decomposition algorithm which can differentiate the five components of the trabecular bone—water, calcium hydroxyapatite, collagen matrix, red marrow, and adipose tissue for each voxel which has been introduced by Nickoloff et al. (16,19).

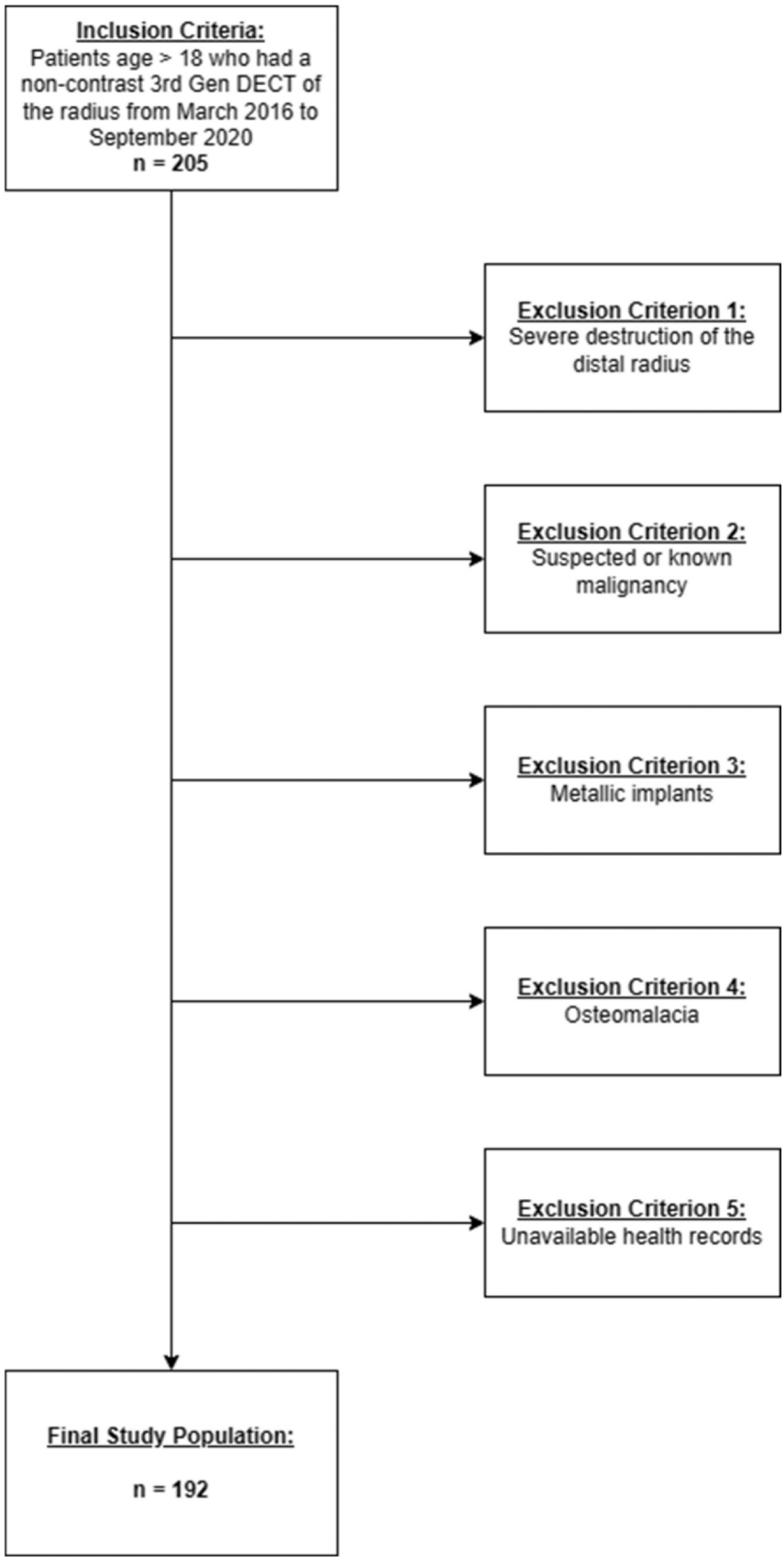

Figure 1. Flow Chart of patient inclusion and exclusion criteria, standards of reporting. 205 patients included, 13 patients excluded, final study population $n = 192$.

Cortical HU, Trabecular HU and Cortical Thickness Ratio

The trabecular HU measurement was based on a HU measurement using the same ROI as for the BMD assessment. The cortical HU was assessed by measuring the HU between the periosteal cortical borders. The cortical thickness ratio was performed as proposed by Rausch et al. (8).

Statistical Analysis

Statistical Analysis was performed with MedCalc (Windows Version 20.1, MedCalc) and R (Windows Version 4.2.2, The R Foundation). To test for normal distribution, the Kolmogorov–Smirnov test was used. Differences in baseline characteristics were evaluated using unpaired t-tests and Mann–Whitney test for continuous variables and Fisher's exact test for categorical values. Data were presented as median with interquartile range in parentheses for age, biological sex, BMD, trabecular HU, cortical HU, cortical thickness ratio. A comparative analysis of the performance of the different metrics in predicting bone-union was performed by ROC curves and PR curves. Pairwise comparison of ROC curves was performed using the DeLong method. Regression analysis was performed using a logistic regression model adjusted for age and female sex to obtain the association of each bone density measurement method (BMD, cortical HU, trabecular HU and cortical thickness ratio) with bone non-union. A p-value < 0.05 was regarded as statistically significant.

RESULTS

Patient Characteristics

A total of 205 patients were considered for study inclusion. 13 patients were excluded due to severe destruction of the distal radius, suspected or known malignancy, metallic implants, osteomalacia, and the unavailability of patient health records. Thus, the study population comprised 192 patients (median age 55 years [IQR 43–67 years]; 108 females, 84 males) **(**Fig 1**)**. Of the 192 DRF patients in our study 20 developed bone non-union. The control group consisted of 172 DRF patients with bone union. Patients who developed bone non-union were significantly older (median age 72 years [IQR 51–74 years]) than those in the control group (median age 54 years [IQR 40–64 years]) **(**Table 1**,** Fig 2**)**. There was no significant difference in fracture severity between the bone non-union patient group and the control group ($p = 0.9$). C fracture was the most common fracture type for the bone non-union group (75% of all fractures in this group) and for the bone union group (74% of all fractures in this group) **(**Table 1**).** DECT-based BMD was significantly lower for patients who developed bone non-union (median BMD 68.1 mg/cm^3 [IQR 62.1–79.5 mg/cm^3]) than for those who did not (median BMD 94.6 mg/cm^3 [IQR, 79.2–110.1 mg/cm^3]), $p < 0.001$. In addition, trabecular HU and cortical HU were not significantly lower for the bone non-union patient group (median trabecular HU, 19.1 HU [IQR −35.5–53.4 HU]; median cortical HU, 1582.5 HU [IQR 1278.8–1769.3 HU]) than in the control group (median trabecular HU 36.5 HU [IQR −18–89 HU]; cortical HU 1710 HU [IQR 1573.5–1842 HU]), $p > 0.05$. The cortical thickness ratio was slightly lower for patients who sustained bone non-union (median cortical thickness ratio 1.33 [IQR 1.28–1.42]) than for those in the control group (1.37 [IQR 1.29–1.45]), $p > 0.05$ **(**Table 1**,** Fig 3**)**.

Logistic Regression Analysis

After adjusting for age and sex, increased DECT-based BMD was significantly associated with lower odds of bone non-union (odds ratio BMD, 0.93 [95% CI: 0.89–0.96], $p < 0.001$). Logistic regression models did not yield significant results for any of the other bone density assessment methods (odds ratio for trabecular HU, 0.99 [95% CI: 0.99–1.01] $p = 0.12$, odds ratio for cortical HU, 0.99 [95% CI: 0.99–1] $p = 0.37$; odds ratio for cortical thickness ratio, 0.2 [95% CI: 0.001–9.67] $p = 0.46$) **(**Table 2**)**.

Comparative Analysis of Measurement Methods via ROC Curves and PR Curves

An optimal DECT-based BMD cut-off value (Youden Index) of 78.1 mg/cm^3 yielded the highest sensitivity (75%) and specificity

TABLE 1. Patient Characteristics Stratified by the Presence or Absence of Bone Union After DRF

Variables	Total DRF (*n* = 192)	Bone Union (*n* = 172)	Bone Non-union (*n* = 20)	P-Value
Age (years)	55 (43, 67)	54 (40, 64)	72 (51, 74)	< 0.001
Male (*n*)	75 (39%)	69 (40%)	6 (30%)	
Female (*n*)	117 (61%)	103 (60%)	14 (70%)	0.53
BMD (mg/cm^3)	91.15 (77.975 -108.2)	94.6 (79.2, - 110.1)	68.1 (62.1 - 79.48)	< 0.001
Trabecular HU	31 (–19.5 - 84.75)	36.5 (–18 - 89)	19.1 (–35.5 - 53.25)	0.14
Cortical HU	1688 (1531.5 - 1837)	1710 (1573.5 - 1842)	1582.5 (1278.75 - 1769.25)	0.06
Cortical thickness ratio	1.36 (1.29 - 1.45)	1.37 (1.29 - 1.45)	1.33 (1.29 - 1.45)	0.41
A Fracture (*n*)	24	24	2	0.9
B Fracture (*n*)	28	27	3	
C Fracture (*n*)	146	127	15	

Note: Bone density assessments are expressed as median with interquartile range in parenthesis. BMD, bone mineral density; DRF, distal radius fracture; HU, Hounsfield Unit; n, number.

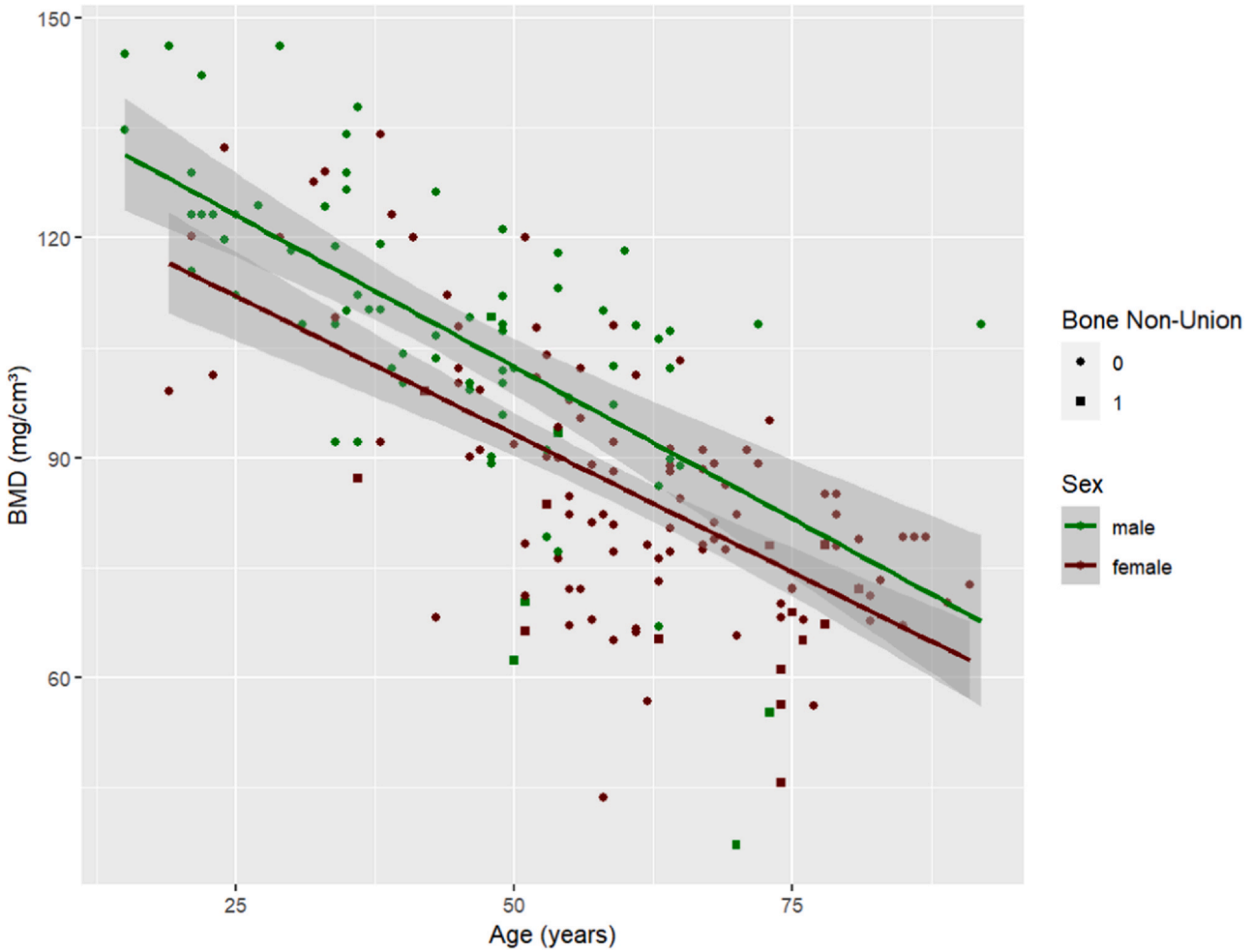

Figure 2. Scatter plot showing volumetric bone mineral density values with and without bone union plotted by age in years of the total study population ($n = 192$). Dark gray area marks 95% confidence interval. BMD, bone mineral density.

(78%) for detecting bone non-union. All other metrics had lower sensitivity and specificity (trabecular HU: cut-off value of 26 HU, sensitivity of 70% and specificity of 54%; cortical HU: cut-off value of 1473 HU, sensitivity of 45%, specificity of 84%, cortical thickness cut-off value of 1.32, sensitivity of 50% and specificity of 64% **(**Fig 4**)**.

A pairwise analysis of the ROC curves revealed that the AUC of DECT-based BMD was significantly higher than the AUC of the other metrics (AUC of DECT-based BMD, 0.83 [95% CI: 73.5–93.1]; AUC of trabecular HU, 0.6 [95% CI 0.48–0.73]; AUC of cortical HU, 0.63 [95% CI 0.49–0.77]; AUC of cortical thickness ratio, 0.56 [95% CI 0.42–0.69] **(**Fig. 4–5**)**.

PR analysis confirmed a higher AUC of DECT-based BMD analysis compared to the other metrics (AUC of DECT-based BMD: 0.46, AUC of cortical HU: 0.16, AUC of trabecular HU: 0.14, AUC of cortical thickness ratio: 0.12) **(**Fig 6**)**.

DISCUSSION

Low BMD is a major risk factor for surgical complications in patients with DRF such as the development of bone non-union (23). The predictive value of DECT-based volumetric BMD assessment for bone non-union in DRF patients has already been demonstrated (22). However, dual-energy CT scanners are not widely available. Therefore, only specialized clinics currently have access to this technique (20). In this retrospective analysis, we compared DECT-based volumetric BMD assessment to various CT-derived metrics obtainable from standard CT devices for their value in predicting bone non-union in patients with DRFs. Our findings show that DECT-based BMD analysis outperforms HU-based metrics and cortical thickness ratio in predicting bone non-union. Unlike the other measurement techniques, only DECT-based BMD assessment yielded a statistically significant prediction model for bone non-union ($p < 0.05$). We adjusted the logistic regression model for age and sex. After adjustment for these covariables increased DECT-based BMD was the sole significant prediction model.

There are several explanations for these findings. Cortical thickness ratio is subject to variability between individuals due to anatomical variations and differences in bone remodeling (24). Furthermore, cortical thickness ratio relies on a simplified, two-dimensional measurement for three-dimensional bone structures. Prior studies have demonstrated that a high proportion of bone marrow and alterations in

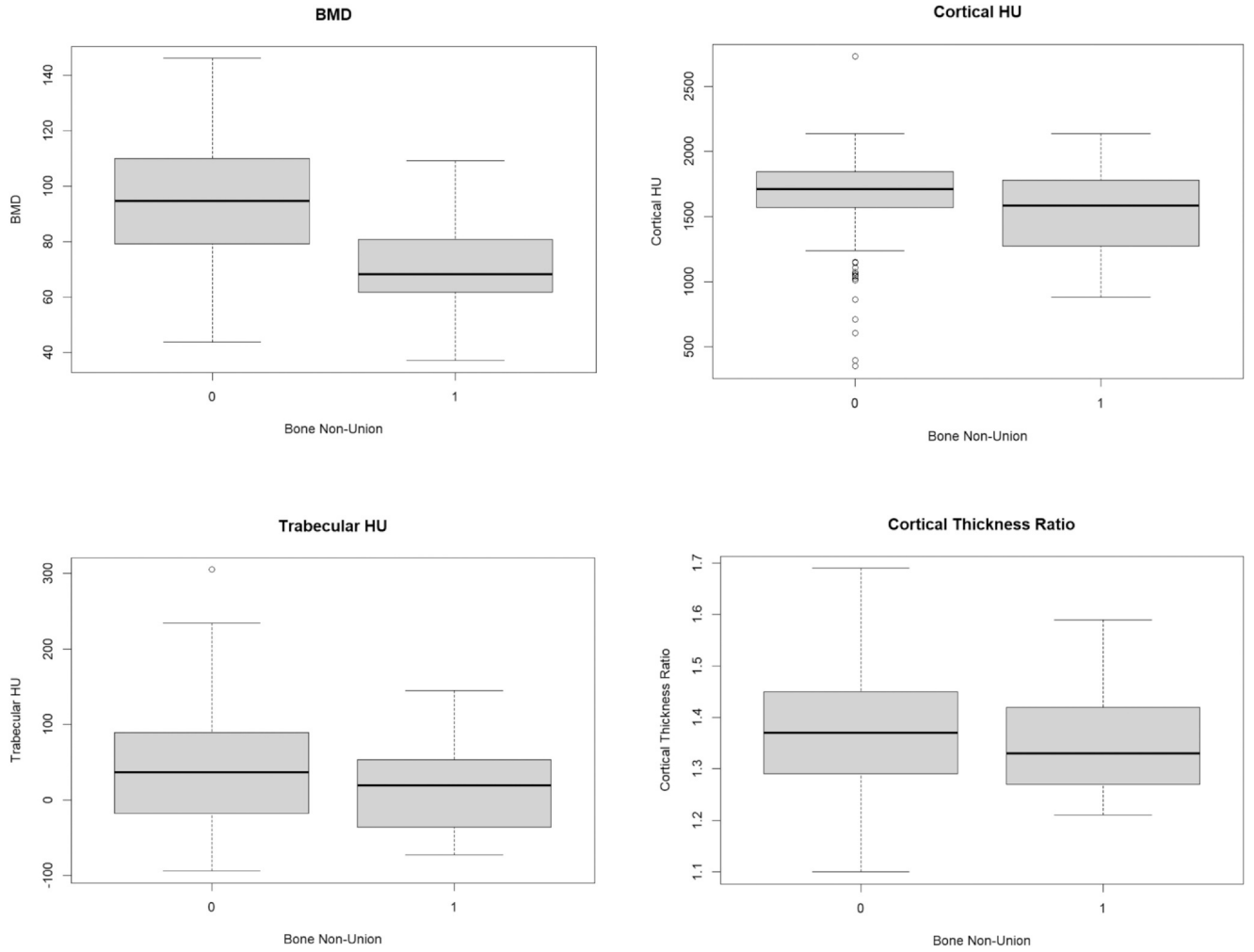

Figure 3. Box plots showing the distribution of values of the different bone density measurement methods with and without bone union. BMD, bone mineral density, HU, Hounsfield Unit.

TABLE 2. Logistic Regression Analysis for the Occurrence of Bone Non-union in DRF

Parameter	Coefficient (β)	Odds Ratio	P-value	*n*
BMD	-0.077	0.926	< 0001	192
Age 50–64	-0.061	0.94	0.049	66
Age 65–79	-0.159	0.853	0.003	40
Age ≥ 80	-0.099	0.906	0.676	13
Female	-0.074	0.929	0.003	117
Cortical HU	-0.001	0.999	0.11	192
Age 50–64	-0.003	0.997	0.029	66
Age 65–79	0	1	0.692	40
Age ≥ 80	0.001	1.001	0.803	13
Female	-0.001	0.999	0.062	117
Trabecular HU	-0.006	0.994	0.118	192
Age 50–64	-0.002	0.998	0.772	66
Age 65–79	-0.003	0.997	0.547	40
Age ≥ 80	0.001	1.001	0.939	13
Female	-0.005	0.995	0.329	117
Cortical thickness ratio	-1.569	0.208	0.456	192
Age 50–64	1.315	3.726	0.706	66
Age 65–79	-4.422	0.012	0.251	40
Age ≥ 80	1.969	7.164	0.856	13
Female	-3.356	0.035	0.211	117

BMD, bone mineral density; HU, Hounsfield Unit.

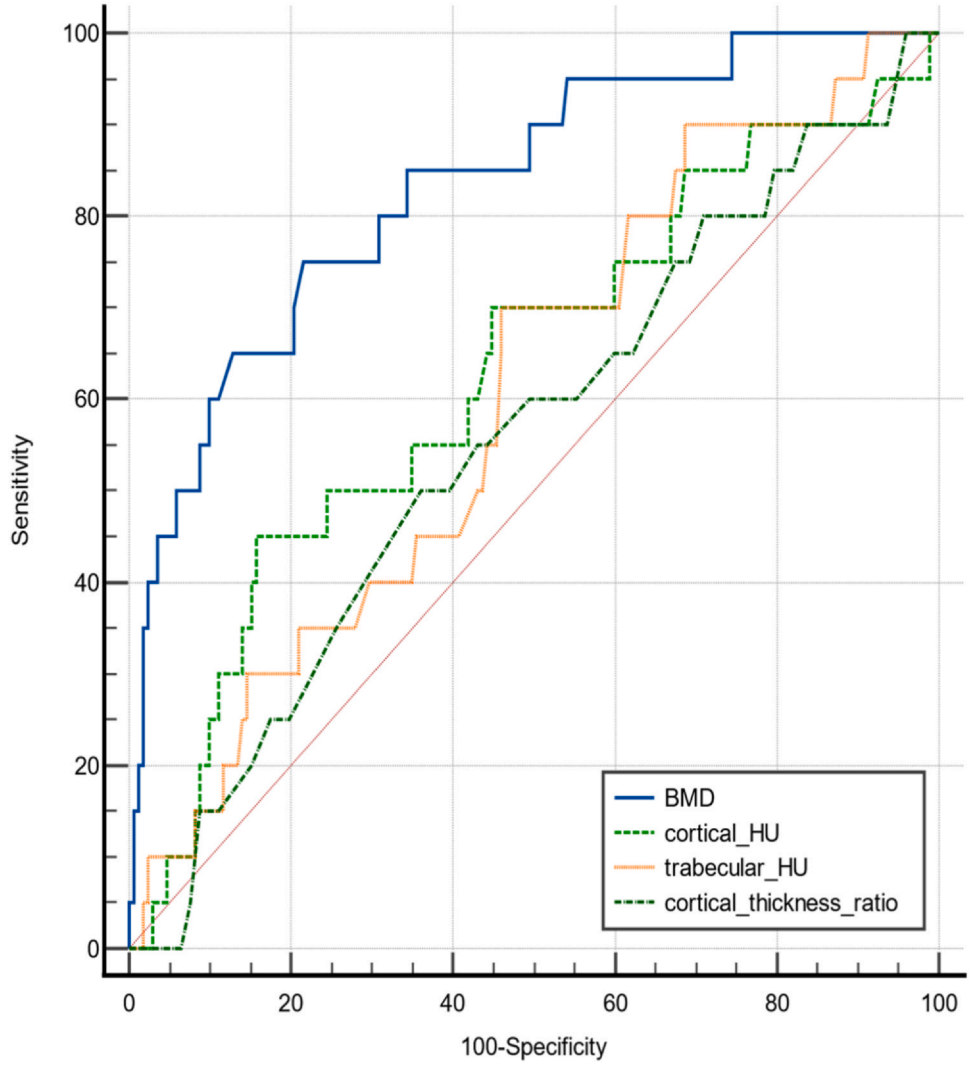

Figure 4. Comparative analysis of the performance of the different bone density measurements in predicting bone-union performed by ROC curves. BMD, bone mineral density; HU, Hounsfield Unit.

body composition are potential sources of inaccuracies for HU-based bone measurement methods. A partial volume effect occurs when bone and the surrounding tissues are included in one voxel which leads to underestimation of BMD (11,25–27).

While the conventional CT does not allow material differentiation, DECT has overcome this limitation. The DECT-based post-processing algorithm enables a three-dimensional material decompensation which adds value in tissue analysis. This algorithm can distinguish compartments of fat, lean, and bone mass accurately with 3D acquisition and analysis (16). Prior research has demonstrated that material decomposition enhances the calculated volumetric BMD in vertebrae by eliminating fat errors (11).

Since the scans in our study were acquired immediately following trauma and prior to treatment initiation the derived BMD data could be integrated into clinical decision-making. DECT examinations contain a high prognostic value for bone non-union risk stratification. The determination of an optimal DECT-based BMD cut-off value of 78.1 mg/cm^3 with corresponding sensitivity of 75% and specificity of 78% adds practical clinical relevance. This cut-off value can guide clinicians in identifying patients at risk for bone non-union.

Given that lower rates of bone union have been reported following internal fixation conservative management could be avoided for patients at risk for bone non-union (28). Furthermore, identifying patients at risk of bone non-union could lead to closer monitoring of fracture healing and close-meshed follow-up controls. Bone non-union often necessitates complex surgical management like bone grafting (29).

Despite these promising findings, several limitations have to be considered. First, approximately 12% of the patients were excluded according to the exclusion criteria, which might introduce a selection bias. Second, all patients were treated at a single hospital, which may limit the generalizability of the findings. Third, a third-generation

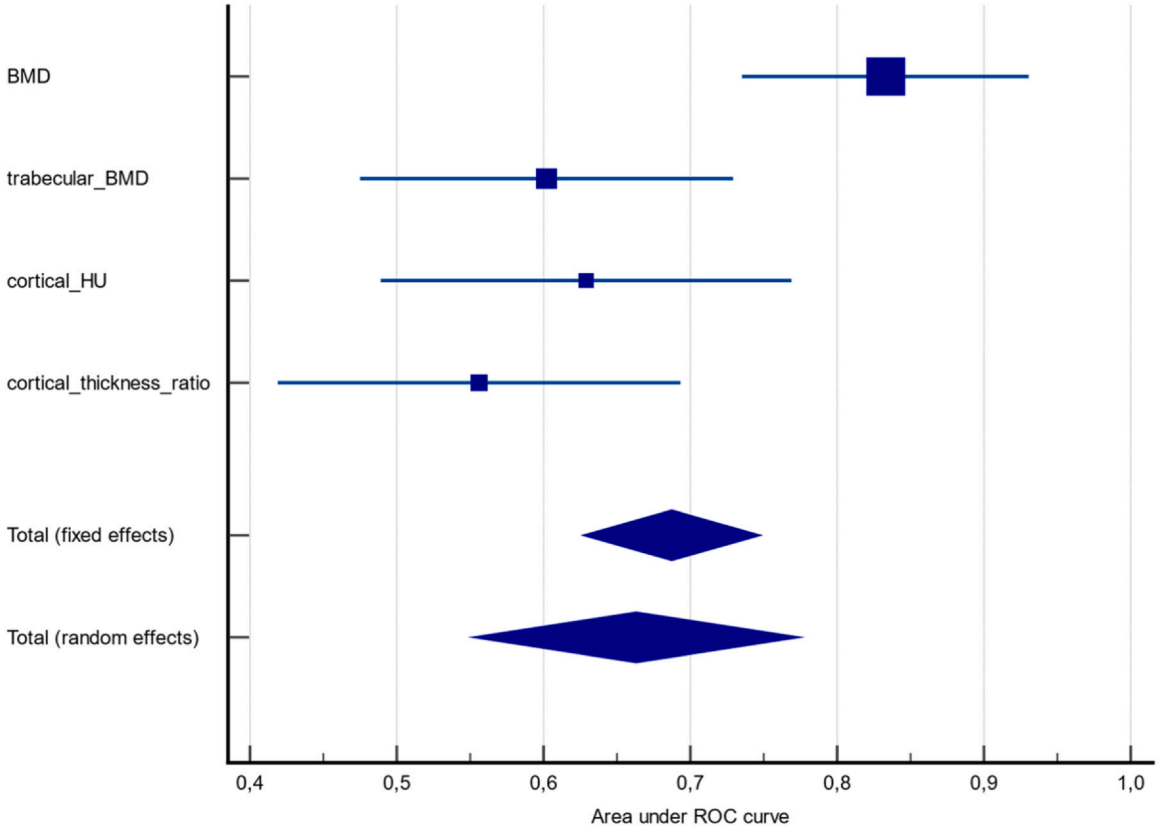

Figure 5. Meta-analysis of the ROC curves of the different bone density measurements in predicting bone-union performed by ROC curves. BMD, bone mineral density; HU, Hounsfield Unit.

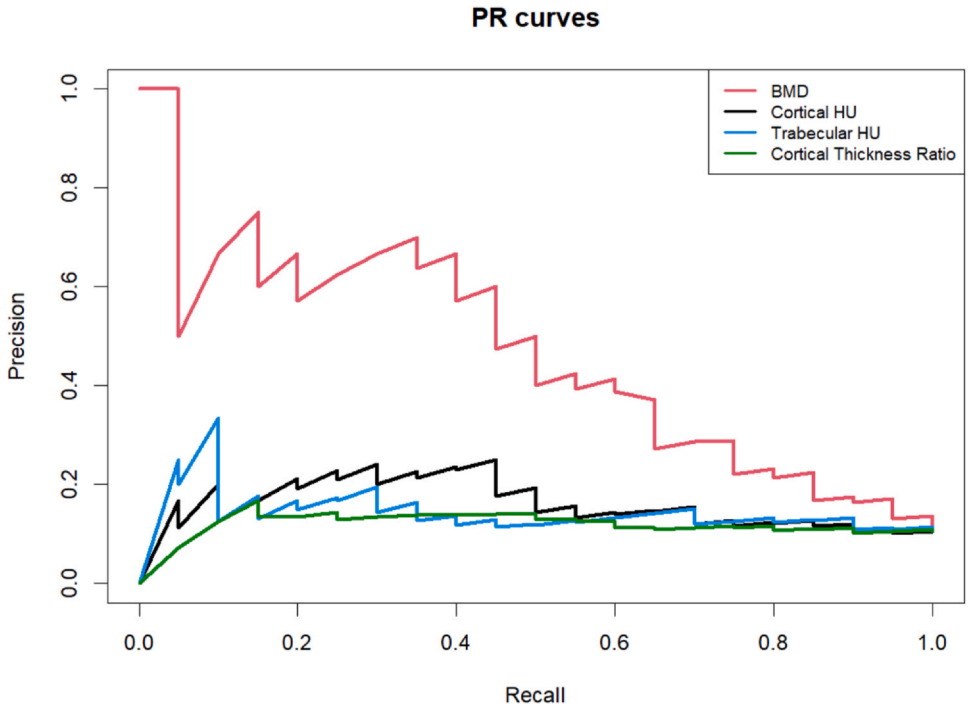

Figure 6. Comparative analysis of the performance of the different bone density measurements in predicting bone-union performed by PR curves.

dual-source CT device might not be available in all healthcare settings limiting the immediate applicability of the study's findings. Fourth, the algorithm used in this work might not be accessible across different hospital systems. Fifth, different acquisition protocols may lead to variations in BMD measurements potentially impacting the accuracy of bone non-union predictions (30). In our study, we used a fixed DECT acquisition protocol to ensure reliable and consistent BMD measurements and thereby improving the accuracy of bone non-union predictions. Sixth, we acknowledge that the AUC values of the PR curve analysis were lower than the AUC values of the ROC curve analysis which might be explained by the imbalanced dataset in our study. However, PR analysis confirmed a higher AUC of DECT-based BMD analysis compared to the other metrics.

As DXA is the current standard method for assessing BMD, future research should compare its performance with that of DECT-based BMD assessment in predicting non-union for DRF (31).

In conclusion, DECT-based BMD showed significantly better diagnostic performance in predicting bone non-union than HU-based metrics and cortical thickness ratio. DECT-based BMD could provide a valuable tool for risk stratification for the occurrence of bone non-union in DRF patients.

DECLARATION OF COMPETING INTEREST

The authors declare that they have no known competing financial interests or personal relationships that could have appeared to influence the work reported in this paper.

REFERENCES

1. Nellans KW, Kowalski E, Chung KC. The epidemiology of distal radius fractures. Hand Clin 2012; 28(2):113–125. https://doi.org/10.1016/j.hcl.2012.02.001
2. Levin LS, Rozell JC, Pulos N. Distal radius fractures in the elderly. J Am Acad Orthop Surg 2017; 25(3):179–187. https://doi.org/10.5435/JAAOS-D-15-00676
3. Shauver MJ, Yin H, Banerjee M, Chung KC. Current and future national costs to medicare for the treatment of distal radius fracture in the elderly. J Hand Surg Am 2011; 36(8):1282–1287. https://doi.org/10.1016/j.jhsa.2011.05.017
4. Edwards BJ, Song J, Dunlop DD, Fink HA, Cauley JA. Functional decline after incident wrist fractures–study of osteoporotic fractures: prospective cohort study. BMJ 2010; 341:c3324. https://doi.org/10.1136/bmj.c3324
5. Lim JA, Loh BL, Sylvestor G, Khan W. Perioperative management of distal radius fractures. 1750458920949463 J Perioper Pract 2021; 31(10). https://doi.org/10.1177/1750458920949463
6. Engelke K, Adams JE, Armbrecht G, et al. Clinical use of quantitative computed tomography and peripheral quantitative computed tomography in the management of osteoporosis in adults: the 2007 ISCD official positions. J Clin Densitom 2008; 11(1):123–162. https://doi.org/10.1016/j.jocd.2007.12.010
7. Pickhardt PJ, Pooler BD, Lauder T, del Rio AM, Bruce RJ, Binkley N. Opportunistic screening for osteoporosis using abdominal computed tomography scans obtained for other indications. Ann Intern Med 2013; 158(8):588–595. https://doi.org/10.7326/0003-4819-158-8-201304160-00003
8. Rausch S, Klos K, Gras F, et al. Utility of the cortical thickness of the distal radius as a predictor of distal-radius bone density. Arch Trauma Res 2013; 2(1):11–15. https://doi.org/10.5812/atr.10687
9. Gruenewald LD, Booz C, Gotta J, et al. Incident fractures of the distal radius: dual-energy CT-derived metrics for opportunistic risk stratification. Eur J Radiol 2024; 171:111283. https://doi.org/10.1016/j.ejrad.2023.111283
10. Mazess RB. Errors in measuring trabecular bone by computed tomography due to marrow and bone composition. Calcif Tissue Int 1983; 35(2):148–152. https://doi.org/10.1007/BF02405022
11. Koch V, Hokamp NG, Albrecht MH, et al. Accuracy and precision of volumetric bone mineral density assessment using dual-source dual-energy versus quantitative CT: a phantom study. Eur Radiol Exp 2021; 5(1):43. https://doi.org/10.1186/s41747-021-00241-1
12. Krug R, Burghardt AJ, Majumdar S, et al. High-resolution imaging techniques for the assessment of osteoporosis. Radiol Clin North Am 2010; 48(3):601–621. https://doi.org/10.1016/j.rcl.2010.02.015
13. Coutts LV, Jenkins T, Oreffo ROC, et al. Local variation in femoral neck cortical bone: in vitro measured bone mineral density, geometry and mechanical properties. J Clin Densitom 2017; 20(2):205–2015. https://doi.org/10.1016/j.jocd.2015.10.003
14. Macdonald HM, Nishiyama KK, Kang J, Hanley DA, Boyd SK. Age-related patterns of trabecular and cortical bone loss differ between sexes and skeletal sites: A population-based HR-pQCT study. J Bone Miner Res 2011; 26(1):50–62. https://doi.org/10.1002/jbmr.171
15. Wesarg S, Kirschner M, Becker M, Erdt M, Kafchitsas K, Khan MF, et al. Dual-energy CT-based assessment of the trabecular bone in vertebrae. Methods Inf Med 2012; 51(5):398–405. https://doi.org/10.3414/ME11-02-0034
16. Nickoloff EL, Feldman F, Atherton JV, Erdt M, Kafchitsas K, F. Khan M. Bone mineral assessment: new dual-energy CT approach. Radiology 1988; 168(1):223–228. https://doi.org/10.1148/radiology.168.1.3380964
17. Gruenewald LD, Koch V, Martin SS, et al. Diagnostic accuracy of quantitative dual-energy CT-based volumetric bone mineral density assessment for the prediction of osteoporosis-associated fractures. Eur Radiol 2022; 32(5):3076–3084. https://doi.org/10.1007/s00330-021-08323-9
18. Gruenewald LD, Koch V, Yel I, et al. Association of phantomless dual-energy CT-based volumetric bone mineral density with the prevalence of acute insufficiency fractures of the spine. Acad Radiol 2022. https://doi.org/10.1016/j.acra.2022.11.020
19. Booz C, Noeske J, Albrecht MH, et al. Diagnostic accuracy of quantitative dual-energy CT-based bone mineral density assessment in comparison to Hounsfield unit measurements using dual x-ray absorptiometry as standard of reference. Eur J Radiol 2020; 132:109321. https://doi.org/10.1016/j.ejrad.2020.109321
20. Zhao W, Lv T, Lee R, Chen Y, Xing L, et al. Obtaining dual-energy computed tomography (CT) information from a single-energy CT image for quantitative imaging analysis of living subjects by using deep learning. Pac Symp Biocomput 2020; 25:139–148.
21. Marsh JL, Slongo TF, Agel J, et al. Fracture and dislocation classification compendium - 2007: orthopaedic trauma association classification, database and outcomes committee. J Orthop Trauma 2007; 21(10):S1–133. https://doi.org/10.1097/00005131-200711101-00001
22. Gruenewald LD, Koch V, Martin SS, et al. Dual-energy CT-based opportunistic volumetric bone mineral density assessment of the distal radius. Radiology 2023; 308(2):e223150. https://doi.org/10.1148/radiol.223150
23. Khalid SI, Nunna RS, Maasarani S, et al. Association of osteopenia and osteoporosis with higher rates of pseudarthrosis and revision surgery in adult patients undergoing single-level lumbar fusion. Neurosurg Focus 2020; 49(2):E6. https://doi.org/10.3171/2020.5.FOCUS20289
24. Goto S, Kataoka K, Isa M, et al. Factors associated with bone thickness: comparison of the cranium and humerus. PLoS One 2023; 18(3):e0283636. https://doi.org/10.1371/journal.pone.0283636
25. Bredella MA, Daley SM, Kalra MK, Brown JK, Miller KK, Torriani M. Marrow adipose tissue quantification of the lumbar spine by using dual-energy CT and single-voxel 1H MR spectroscopy: a feasibility study. Radiology 2015; 277(1):230–235. https://doi.org/10.1148/radiol.2015142876

26. Yu EW, Thomas BJ, Brown JK, Finkelstein JS. Simulated increases in body fat and errors in bone mineral density measurements by DXA and QCT. 10.1002/jbmr.506 J Bone Miner Res 2012; 27(1). https://doi.org/10.1002/jbmr.506
27. Roski F, Hammel J, Mei K, et al. Bone mineral density measurements derived from dual-layer spectral CT enable opportunistic screening for osteoporosis. Eur Radiol 2019; 29(11):6355–6363. https://doi.org/10.1007/s00330-019-06263-z
28. Baertl S, Alt V, Rupp M. Surgical enhancement of fracture healing – operative vs. nonoperative treatment. Injury 2021; 52:S12–S17. https://doi.org/10.1016/j.injury.2020.11.049
29. Fernandez DL, Ring D, Jupiter JB. Surgical management of delayed union and nonunion of distal radius fractures. J Hand Surg Am 2001; 26(2):201–209. https://doi.org/10.1053/jhsu.2001.22917
30. Giambini H, Dragomir-Daescu D, Huddleston PM, Camp JJ, An KN, Nassr A. The effect of quantitative computed tomography acquisition protocols on bone mineral density estimation. J Biomech Eng 2015; 137(11):1145021. https://doi.org/10.1115/1.4031572
31. Jain RK, Vokes T. Dual-energy X-ray absorptiometry. J Clin Densitom 2017; 20(3):291–303. https://doi.org/10.1016/j.jocd.2017.06.014